Available online at www.sciencedirect.com
ScienceDirect
Journal of Sound and Vibration 311 (2008) 1020–1038
JOURNAL OF SOUND AND VIBRATION
www.elsevier.com/locate/jsvi

On the role of fluid viscosity in wave propagation in elastic plates under heavy fluid loading

S.V. Sorokin[a,*], A.V. Chubinskij[b]

[a]Department of Mechanical Engineering, Aalborg University, Pontoppidanstraede 101, DK 9220 Aalborg, Denmark
[b]Department of Mathematics, State Marine Technical University, Lotsmanskaja 3, 190008 St. Petersburg, Russia

Received 11 December 2006; received in revised form 29 September 2007; accepted 1 October 2007
Available online 7 November 2007

Abstract

This paper addresses free wave propagation and attenuation in elastic plates loaded by a quiescent viscous compressible fluid. To validate the adopted fluid model, an elementary problem of wave propagation in a layer of fluid is considered. Then wave propagation in a conventional Kirchhoff plate and in a sandwich plate loaded by a layer of viscous compressible fluid is analysed. The location of dispersion curves in each of these three cases is determined and compared with each other. The viscosity-induced attenuation of otherwise propagating 'fluid-originated' and 'structure-originated' waves is quantified. The parametric studies are conducted to explore the influence of, e.g., the width of a fluid layer or a stiffness ratio of the materials of skin and core plies in a sandwich plate on the wave attenuation.

1. Introduction

The problem of time harmonic linear wave propagation in elastic structures under heavy fluid loading is traditionally considered within the framework of a theory of compressible inviscid fluid (a standard model of the acoustic medium) (see, for example, classical texts [1,2]). This model is perfectly valid for analysis of vibrations of elastic structures submerged into an unbounded volume of the fluid (e.g., a ship hull in water) or vibrations of thin-walled fluid conveying structures (e.g., a water-filled tube). However, in some situations, which are rather typical for various industrial applications (for example, when a capillary is considered), wave propagation occurs in a narrow gap and the attenuation effect produced by viscosity of a fluid cannot be ignored. Other examples of such a situation are narrow slits and small enclosures in hearing aides, small transducers, etc. The regime of fluid motion in these cases is laminar (no mean flow is taken into account) and Navier–Stokes equations may be linearized. Then it is possible to apply a theory suggested in Refs. [3,4] to describe wave motion in a fluid.

Although the effects of fluid viscosity have been carefully studied in relation to sound generation mechanisms in a fluid flowing along the rigid boundary (see, for example, Ref. [5]) the viscosity-induced attenuation of waves travelling in a fluid wave guide has been studied in fewer publications. For example, the wave propagation in a layer of the compressible viscous fluid between absolutely rigid walls has been analysed

*Corresponding author.
E-mail address: svs@ime.aau.dk (S.V. Sorokin).

0022-460X/$ - see front matter © 2007 Elsevier Ltd. All rights reserved.
doi:10.1016/j.jsv.2007.10.001

in Ref. [6] and it has been found that the wave attenuation in water is controlled by Reynolds number, specifically, by the quantity $\sqrt{\nu/\omega H^2}$ (ν is a coefficient of kinematic viscosity, ω is a circular frequency, $2H$ is the width of a fluid layer). This result suggests that propagation of low-frequency purely acoustical waves in a narrow gap filled with water may be substantially suppressed by its viscosity. Apparently, this effect is dramatically amplified for highly viscous fluid as oil, etc.

The replacement of a rigid wall by an elastic structure may substantially change the scenario of wave propagation in a coupled wave-guide in comparison with wave propagation in sub-systems. For example, the acoustic layer between a conventional Kirchhoff plate and a rigid wall (see Ref. [7]), supports only one coupled travelling wave at an arbitrary low frequency, whereas two propagating waves co-exist in sub-systems considered individually (the duct mode in an acoustic layer bounded by rigid walls and the flexural wave in an elastic plate). The fluid–structure interaction conditions in this case involve continuity of normal velocities at the fluid–structure interface and formulation of the contact acoustic pressure as the loading term (distributed transverse force) in the equation of motion of a structure. As soon as the model of a viscous fluid is used, interfacial conditions are formulated for both the normal and the tangential velocity components and fluid loading produces the distributed transverse force and the distributed bending moment acting at the structure. In the case of a conventional thin Kirchhoff plate, the compliance of a plate (the fluid boundary) in tangential direction is relatively small, and these additional interfacial conditions are not dominant.

The situation is quite different in the case of a sandwich plate. As is shown in Ref. [8], a sandwich plate supports propagation of two waves. The first one is of dominantly flexural type and it is similar to its counterpart in a Kirchhoff plate. The second one, which cuts on at a relatively low frequency, is of dominantly shear type (due to the large compliance of a core ply). The amplitude of the tangential velocity component of the surface of skin ply in the course of propagation of this wave may be relatively large and the role of tangential interfacial conditions (which are involved only in the case of viscous fluid) may be dominant.

To the best of the authors' knowledge, the role of effects of fluid viscosity in propagation of low-frequency waves in elastic thin-walled structures under heavy fluid loading produced by a relatively thin layer of the fluid has not been considered in the literature. Therefore, it is expedient to compare the viscosity-induced effects in three above-mentioned model problems of wave propagation in a layer of viscous compressible fluid: when the layer is bounded by rigid walls at both sides, when it is bounded by a rigid wall and a Kirchhoff plate and when it is bounded by a sandwich plate and a rigid wall. Solutions of these problems and discussion of the obtained results constitute the subject of this paper.

Naturally, effects of fluid viscosity play an important role in dynamics of nano- and micro-electro-mechanical systems. Discussion of modelling of propagation of Love and Rayleigh waves in a solid immersed in a viscous fluid may be found in publications related to this area of research (see, for example, Ref. [9] and references provided there). The same holds true as regards use of Reynolds equation for analysis of fluid motion (see Ref. [10]). However, these issues lie well beyond the scope of the present contribution, which is concerned only with analysis of attenuation of relatively low-frequency long waves in fluid-loaded thin plates.

The paper is structured as follows. A model of dynamics of a quiescent viscous fluid is introduced in Section 2. Its application for analysis of wave propagation in a fluid layer between rigid walls (used as a reference case) is presented in the same section. A coupled problem of wave propagation in a Kirchhoff plate loaded by a layer of viscous compressible fluid (with a rigid wall as the second boundary of the layer) is solved in Section 3. A case, when a layer of viscous compressible fluid is bounded at one side by a rigid baffle and by an elastic plate of sandwich composition at another side, is considered in Section 4. Parametric studies of wave attenuation in the case of fluid-loaded sandwich plate are presented in Section 5. Theoretical findings and results of computations reported in the paper are summarized in Section 6.

2. Model of dynamics of quiescent viscous fluid: wave propagation in a rigid duct filled with a viscous compressible fluid

In this paper, the problem of wave propagation in a layer of viscous fluid in the absence of a mean flow is considered. Then it is possible to use linearized Navier–Stokes equations [11,12] to describe dynamics of a fluid

$$\rho_{\mathrm{fl}}\frac{\partial\vec{\mathbf{v}}}{\partial t}-\tilde{\mu}\nabla^2\vec{\mathbf{v}}+\vec{\nabla}p-(\lambda+\tilde{\mu})\vec{\nabla}(\vec{\nabla}\cdot\vec{\mathbf{v}})=0, \tag{1}$$

$$\frac{\partial \rho}{\partial t} + \rho_{\mathrm{fl}} \vec{\nabla} \cdot \vec{\mathbf{v}} = 0, \tag{2}$$

$$\hat{\boldsymbol{\sigma}} = \left(-p + \lambda \vec{\nabla} \cdot \vec{\mathbf{v}}\right) \hat{\mathbf{E}} + 2\tilde{\mu} \hat{\mathbf{e}},$$

$$2\hat{\mathbf{e}} = \vec{\nabla} \vec{\mathbf{v}} + \left(\vec{\nabla} \vec{\mathbf{v}}\right)^{\mathrm{T}}, \tag{3}$$

$$\frac{\partial p}{\partial \rho} = c_{\mathrm{fl}}^2, \tag{4}$$

where ρ_{fl} is the fluid density, c_{fl} is the sound speed, p is the pressure perturbation, ρ is the density perturbation, $\vec{\mathbf{v}}$ is the velocity vector, $\hat{\boldsymbol{\sigma}}$ and $\hat{\mathbf{e}}$ are the stress and strain rate tensors, $\hat{\mathbf{E}}$ is a unit tensor, $\tilde{\mu}$ and v are dynamic and kinematic coefficients of viscosity, $\tilde{\mu} = \rho_{\mathrm{fl}} v$, λ is the second coefficient of viscosity and $\lambda = -\frac{2}{3}\widehat{\mu}$ (see Ref. [12]).

The velocity field is sought in the following form (this formulation is similar to its counterpart in the theory of elasticity and it has been used in Refs. [3,4]):

$$\vec{\mathbf{v}} = \vec{\nabla} \varphi + \vec{\nabla} \times \vec{\boldsymbol{\psi}}. \tag{5}$$

In the plane problem formulation (z is the vertical axis and x is the horizontal axis as shown in Fig. 1), $\psi_x = \psi_z = 0$, so that $\psi \equiv \psi_y$

$$v_x = \frac{\partial \varphi}{\partial x} - \frac{\partial \psi}{\partial z}, \quad v_z = \frac{\partial \varphi}{\partial z} + \frac{\partial \psi}{\partial x}. \tag{6}$$

The potentials φ and ψ [3,4] satisfy uncoupled equations:

$$\left[\left(1 + \frac{4\hat{\mu}}{3\rho_{\mathrm{fl}} c_{\mathrm{fl}}^2} \frac{\partial}{\partial t}\right) \nabla^2 - \frac{1}{c_{\mathrm{fl}}^2} \frac{\partial^2}{\partial t^2}\right] \varphi = 0, \tag{7}$$

$$\left(v \nabla^2 - \frac{\partial}{\partial t}\right) \psi = 0. \tag{8}$$

Then the pressure is expressed only via the scalar potential:

$$p = \rho_{\mathrm{fl}} \left(\frac{4\hat{\mu}}{3\rho_{\mathrm{fl}}} \nabla^2 - \frac{\partial}{\partial t}\right) \varphi. \tag{9}$$

Normal and shear stresses are formulated as

$$\sigma_{zz} = -p + 2\widehat{\mu} \frac{\partial v_z}{\partial z}, \tag{10}$$

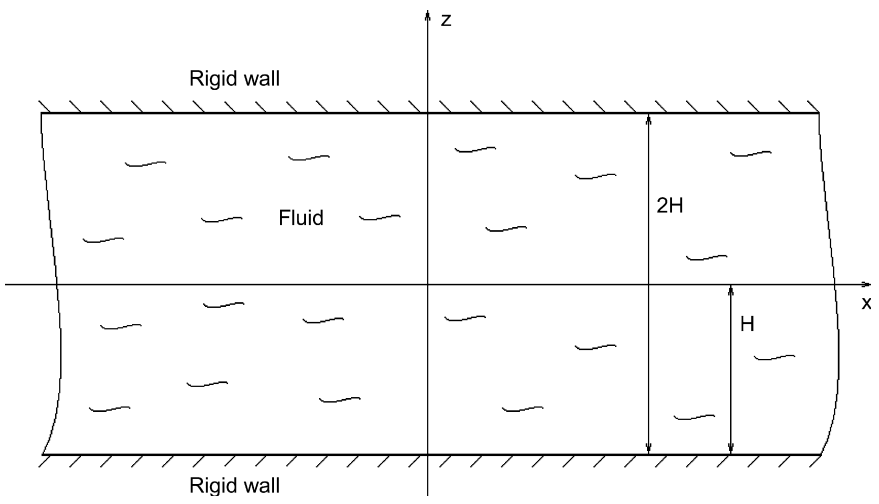

Fig. 1. A fluid layer between rigid walls.

$$\tau_{zx} = \widehat{\mu}\left(\frac{\partial v_z}{\partial x} + \frac{\partial v_x}{\partial z}\right). \tag{11}$$

Taking into account Eqs. (6) and (9), two last equations are written as

$$\sigma_{zz} = -\rho_{\mathrm{fl}}\left(\frac{4\nu}{3}\nabla^2 - \frac{\partial}{\partial t}\right)\varphi + \rho_{\mathrm{fl}}\nu\left(\frac{\partial^2\varphi}{\partial z^2} + \frac{\partial^2\psi}{\partial x\,\partial z}\right), \tag{12}$$

$$\tau_{xz} = \rho_{\mathrm{fl}}\nu\left(2\frac{\partial^2\varphi}{\partial x\,\partial z} - \frac{\partial^2\psi}{\partial z^2} + \frac{\partial^2\psi}{\partial x^2}\right). \tag{13}$$

To study the influence of viscosity on propagation of waves in the fluid layer bounded by rigid walls, boundary conditions at their surfaces are formulated as

$$z = \pm H \quad \begin{cases} v_x = \dfrac{\partial\varphi}{\partial x} - \dfrac{\partial\psi}{\partial z} = 0, \\ v_z = \dfrac{\partial\varphi}{\partial z} + \dfrac{\partial\psi}{\partial x} = 0 \end{cases} \tag{14}$$

(the thickness of viscous fluid layer is $2H$, see Fig. 1).

Solution of system (7), (8) and (14) is sought in the form

$$\varphi = A(z)\exp(kx - \mathrm{i}\omega t),\ \psi = B(z)\exp(kx - \mathrm{i}\omega t). \tag{15}$$

In what follows, Eq. (7) is simplified by neglecting the second term, which contains the second viscosity, $4\hat{\mu}/3\rho_{\mathrm{fl}}c_{\mathrm{fl}}^2$. Then the conventional wave equation describes behaviour of the velocity potential φ. Standard algebra gives the following dispersion equation in the non-dimensional form:

$$(\alpha\beta\cos\alpha\sin\beta - K^2\sin\alpha\cos\beta)(\alpha\beta\sin\alpha\cos\beta - K^2\cos\alpha\sin\beta) = 0. \tag{16}$$

Here following notations are introduced:

$$\alpha = \sqrt{K^2 + \Omega^2},\quad \beta = \sqrt{K^2 + \mathrm{i}\frac{\Omega}{\mu}},\quad K = kH,\quad \Omega = \frac{\omega H}{c_{\mathrm{fl}}},\quad \mu = \frac{\nu}{c_{\mathrm{fl}}H}. \tag{17}$$

The factorized structure of dispersion equation (16) highlights the existence of symmetric and skew-symmetric modes, which naturally follows from the symmetry of the layer with respect to the x-axis (see Fig. 1).

The dispersion equation for symmetric modes is

$$\sqrt{K^2+\Omega^2}\,\sin\left(\sqrt{K^2+\Omega^2}\right) - \frac{K^2}{\sqrt{K^2+\mathrm{i}\Omega/\mu}}\cos\left(\sqrt{K^2+\Omega^2}\right)\frac{\sin\left(\sqrt{K^2+\mathrm{i}\Omega/\mu}\right)}{\cos\left(\sqrt{K^2+\mathrm{i}\Omega/\mu}\right)} = 0. \tag{18}$$

In the case $O(K)\sim O(\Omega)\sim\mu^0$, it is convenient to introduce the following scaling $K = \tilde{K}\mu^0$ and $\Omega = \tilde{\Omega}\mu^0$, where $\tilde{K}\sim\tilde{\Omega}\sim 1$. In the limit $\mu\to 0$, Eq. (18) is reduced to

$$\sqrt{\tilde{K}^2+\tilde{\Omega}^2}\,\sin\left(\sqrt{\tilde{K}^2+\tilde{\Omega}^2}\right) - \mathrm{i}\sqrt{\frac{\mu}{\mathrm{i}\tilde{\Omega}}}\tilde{K}^2\cos\left(\sqrt{\tilde{K}^2+\tilde{\Omega}^2}\right) = 0. \tag{19}$$

Then the wavenumber of a propagating wave may be presented explicitly as

$$K \approx \mathrm{i}\Omega\left(1 + \frac{1}{2}\sqrt{\frac{\mu}{2\Omega}}(1+\mathrm{i}) + \mathrm{i}\mu\left(\frac{3}{8\Omega} + \frac{1}{4}\Omega\right)\right). \tag{20}$$

The solution of this problem reported in Ref. [6] is the same up to $\sqrt{\mu}$-order term.

The second cut-on frequency of symmetric modes is defined when the condition $K = 0$ is applied in Eq. (18) and resulting equation is solved with respect to $\Omega_{\text{cut-on}}$. It yields $\Omega_{\text{cut-on},2}^{\text{sym}} = \pi$.

The dispersion equation for skew-symmetric waves is asymptotically reduced as

$$\sqrt{\tilde{K}^2+\tilde{\Omega}^2}\cos\left(\sqrt{\tilde{K}^2+\tilde{\Omega}^2}\right)+\mathrm{i}\sqrt{\frac{\mu}{\mathrm{i}\tilde{\Omega}}}\tilde{K}^2\sin\left(\sqrt{\tilde{K}^2+\tilde{\Omega}^2}\right)=0. \tag{21}$$

It is easy to check, that there are no propagating skew-symmetric modes in low-frequency range up to $\Omega^{\mathrm{skew}}_{\text{cut-on},1}=\pi/2$. This cut-on frequency is found exactly in the same manner as the second cut-on frequency of symmetric propagating modes.

In the elementary case of the acoustic layer between rigid walls ($\mu=0$), dispersion equation (16) acquires the familiar form

$$\sin 2\sqrt{K^2+\Omega^2}=0. \tag{22}$$

Naturally, its factorization yields the dispersion equation for the symmetric (with respect to the axis x, see Fig. 1) modes

$$\sin\sqrt{K^2+\Omega^2}=0 \tag{23a}$$

and for skew-symmetric ones,

$$\cos\sqrt{K^2+\Omega^2}=0. \tag{23b}$$

Dispersion curves defined by these equations are well-known. As is seen from comparison of Eqs. (18), (21) and (22) in the case $K=0$, magnitudes of cut-on frequencies $\Omega^{\mathrm{sym}}_{\text{cut-on},2}$, $\Omega^{\mathrm{skew}}_{\text{cut-on},1}$ are not affected by viscosity.

These dispersion equations, as well as all other ones solved in this paper, have infinitely many, in general, complex-valued roots for any frequency parameter Ω. The methodology of their computation suggested in Ref. [8] is adopted here. In effect, the original dispersion equation is replaced by its polynomial counterpart, which is easily obtained when trigonometric functions are replaced by their polynomial approximations. Apparently, the order of an approximate polynomial dispersion equation is controlled by the number of terms retained in power series. Then all roots of this approximate polynomial dispersion equation can easily be found by use, for example, Mathematica [13] symbolic manipulator. Furthermore, this manipulator is used to search for roots of the original dispersion equation with the 'initial guesses' taken as roots of approximate dispersion equation. These roots are selected in the following way: $\mathrm{Re}\,(K_l)<0$, or, if $\mathrm{Re}\,(K_l)=0$, then $\mathrm{Im}\,(K_l)>0$. This selection is based on the formulation of Sommerfeld radiation condition at infinity for purely imaginary roots (time dependence is set to be $\exp(-\mathrm{i}\omega t)$) and decay condition for complex-valued and purely real roots.

The influence of the viscosity on shape and location of dispersion curves is relatively weak: as is seen from Eq. (20), the difference between wavenumber K in acoustic and viscous cases is of order $\sqrt{\mu}$ for given Ω. Since the paper is concerned with wave propagation in elastic plates under heavy fluid loading, the detailed analysis of dispersion curves for the fluid layer between rigid walls is not conducted here. However, this elementary case is referenced in subsequent sections.

The simple result (20) suggests that the analysis of location of dispersion curves and of wave attenuation can conveniently be split into two parts. The first one is to determine the leading order term in expansion of the wavenumber K on the viscosity parameter μ. For this purpose, it is sufficient to consider an ideal acoustic medium, i.e., to set $\mu=0$. At this stage, it is useful to identify all propagating modes and to classify them as structure- or fluid-originated ones. The second step of analysis is to assess the viscosity-induced attenuation of these waves. As soon as the model of a viscous compressible fluid is used, the wave, which propagates in an ideal acoustic medium, transforms to the 'almost propagating' (attenuated) type, so that its wavenumber K becomes complex, i.e., it acquires a negative real part, as seen in Eq. (20). The magnitude of the real part of K vanishes as viscosity parameter tends to zero, $\mu\to 0$. To illustrate this effect, it is natural to explore the dependence of real parts of K upon Ω for these 'almost propagating' waves. Another measure of wave attenuation is the ratio of the amplitude of an out-coming wave to the amplitude of an incoming wave as is passes in x-direction along the layer of a given length (see Fig. 1). Naturally, these two measures are linked to each other.

The remaining sections of this paper are structured in accordance with this formulation of sub-tasks. The solutions of problems of wave propagation in a Kirchhoff plate and in a sandwich plate loaded with a viscous compressible fluid are reported along with studies of the location of dispersion curves, which is virtually the same as in the case, when fluid loading is produced by an acoustic medium. The parametric studies of the viscosity-induced effects (which may be characterized as 'zooming in' branches of dispersion curves) for a Kirchhoff plate and for a sandwich plate are put together in a separate section to facilitate their comparison.

3. Wave propagation in a Kirchhoff plate loaded by a layer of viscous compressible fluid

The problem of wave propagation in an elastic plate loaded by an unbounded volume of the acoustic medium may be regarded as a classical problem in vibro-acoustics [1,2]. Recent advances in modelling wave propagation in elastic fluid-loaded plates within this problem formulation are reported in Refs. [14–17]. However, in some situations outlined in Section 1 fluid loading is produced by a fluid layer. The wave propagation problem in this case has been solved by Fahy [18] for a Kirchhoff plate loaded by a layer of the acoustic medium. The same problem for a fluid-loaded sandwich plate has been solved in Ref. [8]. An asymptotic analysis of results reported in Ref. [18] has been performed recently in Ref. [19].

As the thickness of the layer becomes 'sufficiently' small, one could expect viscous effects in the fluid (e.g., water) to become increasingly important. To assess the level, to which viscosity may alter the fluid–structure interaction in comparison with the situation, when effects of viscosity are neglected, consider a model problem for a plate in 'cylindrical bending' (see Fig. 2). An infinitely long Kirchhoff plate is loaded by a layer of viscous compressible fluid. This layer has the thickness $2H$ and it is bounded by a rigid wall at the opposite to the plate side. The equation of motion of a plate ($w(x,t)$ is the transverse displacement of mid-surface of the plate) is formulated as [20]:

$$D_1 \frac{\partial^4 w}{\partial x^4} + M \frac{\partial^2 w}{\partial t^2} = -\sigma_{zz} + \frac{\partial m}{\partial x}, \tag{24}$$

$$D_1 = \frac{Eh^3}{12(1-\nu_p^2)} = Eh^3 \tilde{D}_1, \quad M = \rho_{\mathrm{pl}} h, \tag{25}$$

where E is Young's modulus, ν_p is Poisson's ratio, ρ_{pl} is density and h is the thickness of a plate.

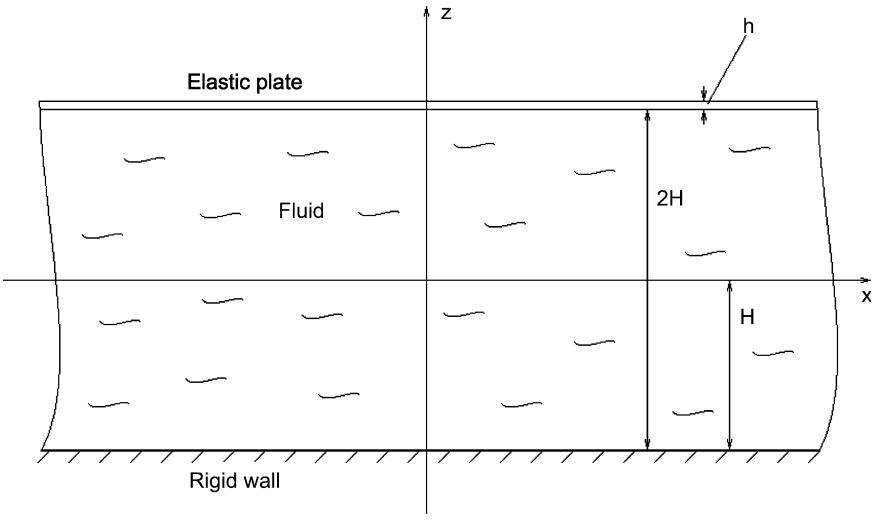

Fig. 2. A fluid-loaded conventional plate.

As is seen from Eq. (24), viscous fluid produces both the conventional distributed transverse force at the surface of a plate and the distributed bending moment,

$$m = \frac{h}{2}\tau_{zx}. \tag{26}$$

Apparently, it vanishes as soon as the standard model of an acoustic medium is adopted.

Dynamics of the fluid is governed by Eqs. (7) and (8), with two continuity conditions at the fluid–structure interface, $z = H$

$$\begin{cases} v_x = \dfrac{\partial\varphi}{\partial x} - \dfrac{\partial\psi}{\partial z} = \dfrac{h}{2}\dfrac{\partial^2 w}{\partial t\,\partial x}, \\ v_z = \dfrac{\partial\varphi}{\partial z} + \dfrac{\partial\psi}{\partial x} = \dfrac{\partial w}{\partial t}. \end{cases} \tag{27}$$

The second pair of conditions at $z = -H$ is the same as in the previous case.

A solution of the problem (7),(8) and (24)–(27) is sought in the form

$$\varphi = A(z)\exp(kx - \mathrm{i}\omega t), \quad \psi = B(z)\exp(kx - \mathrm{i}\omega t), \quad w = D\exp(kx - \mathrm{i}\omega t). \tag{28}$$

Standard algebra gives the following dispersion equation in non-dimensional form:

$$T_1 - \frac{\mathrm{i}P\Omega\mu}{48S}T_2 = 0. \tag{29}$$

It is solved by the same method as Eqs. (18), (19) and (21). Cumbersome coefficients involved in Eq. (29) can be found in the Appendix.

Dispersion curves are presented in Fig. 3a and b for the following set of parameters: $\mu = 10^{-6}$, $0.01 \leqslant \Omega \leqslant 0.6$, $\nu_p = 0.3$, $P = 0.128$, $\Delta = 3.258$, $\chi = 10$ ($\chi = H/h$, $P = \rho_{\mathrm{fl}}/\rho_{\mathrm{pl}}$, $\Delta = c_{\mathrm{pl}}/c_{\mathrm{fl}}$), which is typical for the combination 'steel-water'. As already discussed, graphs shown in these figures are almost identical to those plotted for the same plate loaded by the layer of an inviscid compressible fluid ($\mu = 0$) of the same density. The dispersion equation for such a plate can be found, for instance, in Refs. [7,18,19]. It has the following form

$$T_1 + P\Omega^2\frac{\cot(2\sqrt{K^2+\Omega^2})}{\sqrt{K^2+\Omega^2}} = 0. \tag{30}$$

For the given combination of parameters, the real part of a complex-valued wavenumber of the 'almost propagating wave' is very small in comparison with real parts of the wavenumbers of 'authentically' decaying waves. Therefore, all dispersion curves shown in Fig. 3a and b may be attributed to the plate loaded by the acoustic layer. Location of these curves is studied hereafter, whereas the wave attenuation due to fluid viscosity is considered in Section 5 for all three models (fluid layer, Kirchoff plate and sandwich plate under heavy fluid loading).

Real and imaginary parts of roots of dispersion Eq. (30) versus frequency parameter are shown in Fig. 3a and b. Propagating waves ('almost propagating' waves in the case of a viscous fluid) are presented by curves 1 and 10. All other curves in this figure present evanescent waves. For example, curve 2 in Fig. 3a presents the negative real part of the pair of complex conjugate roots with imaginary parts shown as curves 2a and b in Fig. 3b. At $\Omega \approx 0.06$ this pair of complex conjugate roots splits into branches 3 and 4. In the case of an acoustic medium, they specify purely real roots. In the case of a viscous fluid, these roots acquire sufficiently small imaginary parts. Then branches 4 and 5 merge into branch 6 at $\Omega \approx 0.11$. Branch 6 in Fig. 3a presents the real part of two complex conjugate roots with imaginary parts shown as branches 6a and 6b in Fig. 3b. At $\Omega \approx 0.50$ these roots become purely real again and branch 6 splits into branches 7 and 8. Then scenario repeats itself as frequency parameter grows. At $\Omega \approx 0.58$ curve 3 in Fig. 3a attains zero. This is the cut-on frequency, at which the corresponding mode transforms from the evanescent to the propagating type. This emerged propagating (in the case of an acoustic medium) wave is presented by curve 10 in Fig. 3b. In the case of a viscous fluid, curve 10 in Fig. 3b presents the imaginary part of a complex-valued wavenumber. Its real part is presented by curve 10 in Fig. 3a, which is virtually non-distinguishable from the coordinate axis.

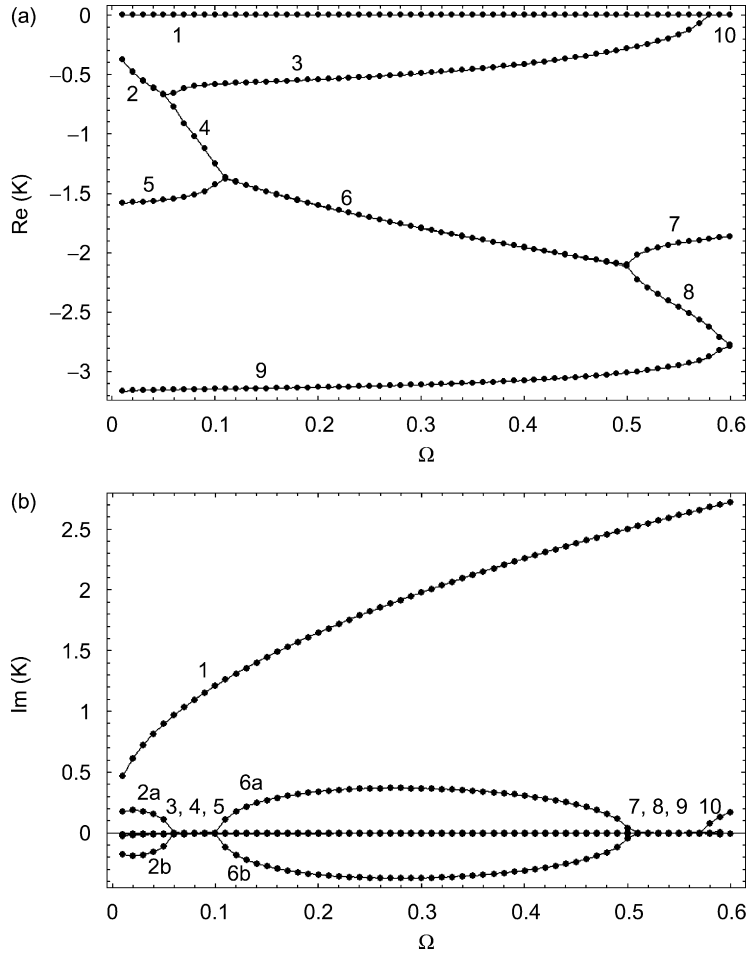

Fig. 3. Dispersion curves for a fluid-loaded conventional plate: (a) real parts and (b) imaginary parts.

As mentioned, the 'zoomed-in' graphs presenting the negative real parts of otherwise purely imaginary roots are displayed in Section 5.

The magnitudes of cut-on frequencies are readily found by setting $K = 0$ in dispersion Eq. (30). The equation, which defines cut-on frequencies, is

$$-\frac{\Omega^2}{\chi} + P\sqrt{\Omega^2}\,\cot(2\sqrt{\Omega^2})\frac{3 - 2i\mu\Omega}{3} = 0. \tag{31}$$

Its counterpart for a layer of viscous fluid between rigid walls is readily obtained from Eq. (16)

$$\sin 2\Omega \sin 2\sqrt{\frac{i\Omega}{\mu}} = 0. \tag{32}$$

If viscosity is neglected, cut-on frequencies for the layer of an acoustic medium between rigid walls are defined by equation

$$\sin 2\Omega = 0. \tag{33}$$

Finally, for the waveguide shown in Fig. 2 Eq. (31) is reduced as

$$-\frac{\Omega^2}{\chi} + P\sqrt{\Omega^2}\,\cot(2\sqrt{\Omega^2}) = 0. \tag{34}$$

The first cut-on frequency found from Eq. (34) is $\Omega \approx 0.5745$, whereas solution of Eq. (31) gives $\Omega \approx 0.5745 + 0.000000108I$. Discrepancy in the magnitude of the real part of $\Omega_{\text{cut-on}}$ is of the same order as the magnitude of its imaginary part for a viscous fluid. Naturally, this observation holds true for the difference in magnitudes of wavenumbers calculated at the same frequency for a viscous compressible fluid and for an acoustic medium.

It is expedient to identify modes in the coupled wave guide by overlapping dispersion curves for the plate loaded by the fluid layer, for the plate in vacuum and for the fluid layer between two rigid walls as is shown in Fig. 4a and b. Curves denoted by boxes (A1–A3) correspond to the 'rigid duct' case, curves denoted by daggers (B1 and B2)—to the 'dry Kirchhoff plate' case. Curve A1 correspond to the propagating mode and curves A2 and A3—to evanescent ones. Curves B1 and B2 presents the propagating and the evanescent mode, respectively. Curves designated by dots are the same as in Fig. 3a and b (with the same numeration of branches).

As is seen from Fig. 4a and b, each branch of dispersion curves for a coupled system may be identified either as a structure-originated or as a fluid-originated one. For example, dispersion curve 1 may be called structure-originated and its location is influenced by the presence of a fluid relatively weakly. However, the first propagating 'rigid duct mode' is suppressed in a coupled wave guide. This effect is produced by the fluid–structure interaction rather than fluid viscosity and it is in a contrast with the influence of compliant wall on propagation of 'rigid duct mode' in an elastic cylindrical shell. Deformation of the shell's wall in the

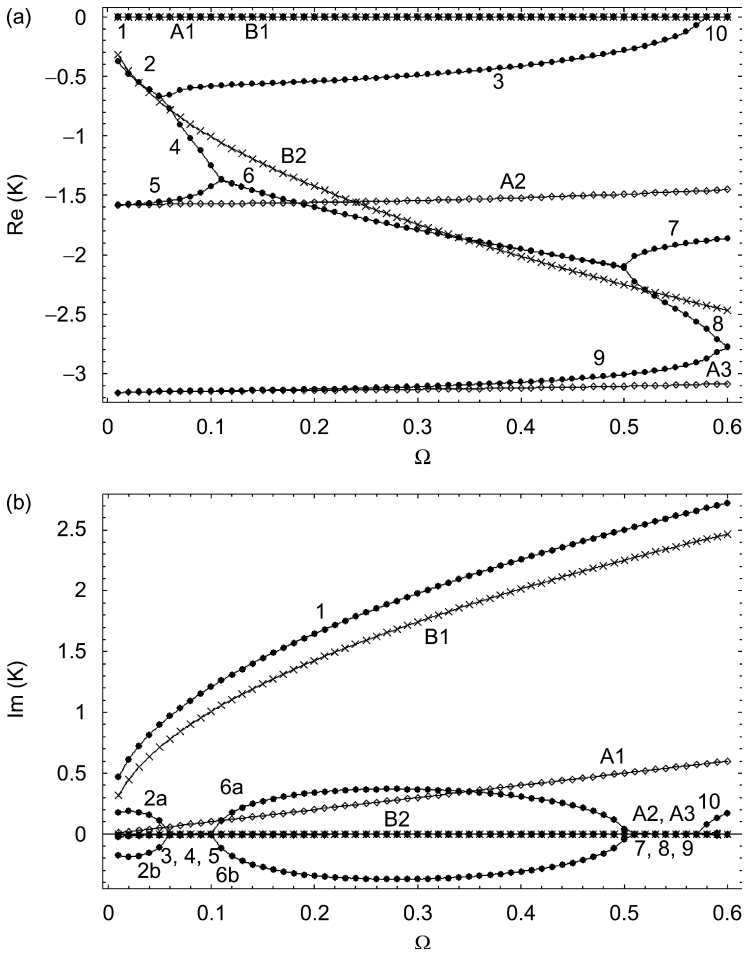

Fig. 4. Dispersion curves for a fluid-loaded plate versus their counterparts in uncoupled cases: (a) real parts and (b) imaginary parts.

circumferential direction produced by the pressure in the shell's 'breathing mode' makes propagation of this 'fluid-originated' mode possible. In the case of a fluid-loaded plate in cylindrical bending considered here, the out-of-plane deformation is constrained and therefore this mode cannot propagate at low frequencies if the wall is compliant. However, other 'fluid-originated modes' (which propagate in a fluid layer when the excitation frequency exceeds its cut-on value) are not suppressed by the compliance of a plate. Moreover, their cut-on frequencies are lowered as can be seen in comparison of locations of curve A2 and 3 in Fig. 4a and curve 10 (which is a continuation of curve 3) in Fig. 4b. The branches A2 and B2, which represent decaying waves in sub-systems, interact with each other so that their counterparts undergo several transformations in the 'intersection' frequency range. Apparently, the set of curves 2, 4, 6 and 8 represent the structure-originated evanescent mode (B2) and the set of curves 5–7 represent the fluid-originated evanescent mode A2.

4. Wave propagation in a sandwich plate loaded by a layer of viscous compressible fluid

An infinitely long sandwich plate is loaded by a layer of viscous compressible fluid. This layer has the thickness $2H$ and it is bounded by a rigid wall at the opposite to a plate side as shown in Fig. 5. The sandwich plate consists of two symmetrical relatively thin, stiff skin plies and thick, compliant core ply. Dimensionless parameters are introduced to describe the internal structure of sandwich plate: $\varepsilon = h_{\text{skin}}/h_{\text{core}}$ as the thickness parameter (the ratio of thickness of each individual skin ply to the thickness of a core ply), $\delta = \rho_{\text{core}}/\rho_{\text{skin}}$ as the density parameter, $\gamma = E_{\text{core}}/E_{\text{skin}}$ as the longitudinal stiffness parameter and $\gamma_g = G_{\text{core}}/G_{\text{skin}}$ as the shear stiffness parameter. Hereafter, subscripts denoting parameters of skin plies are omitted. All plies are assumed to be isotropic, $\gamma = \gamma_g$.

The deformation of a sandwich plate element is governed by two independent variables: a displacement of the mid-surface w (which is the same for all plies) and a shear angle between the mid-surfaces of skin plies θ. Dynamics of a fluid-loaded plate is governed by following equations [8]:

$$D_1 \frac{\partial^4 w}{\partial x^4} - \Gamma\left(\frac{\partial \theta}{\partial x} + \frac{\partial^2 w}{\partial x^2}\right) + M\frac{\partial^2 w}{\partial t^2} - I_1 \frac{\partial^4 w}{\partial x^2 \partial t^2} = -\sigma_{zz} + N_1 \frac{\partial \tau_{zx}}{\partial x}, \tag{35a}$$

$$-D_2 \frac{\partial^2 \theta}{\partial x^2} + \Gamma\left(\theta + \frac{\partial w}{\partial x}\right) + I_2 \frac{\partial^2 \theta}{\partial t^2} = -N_1 \tau_{zx}. \tag{35b}$$

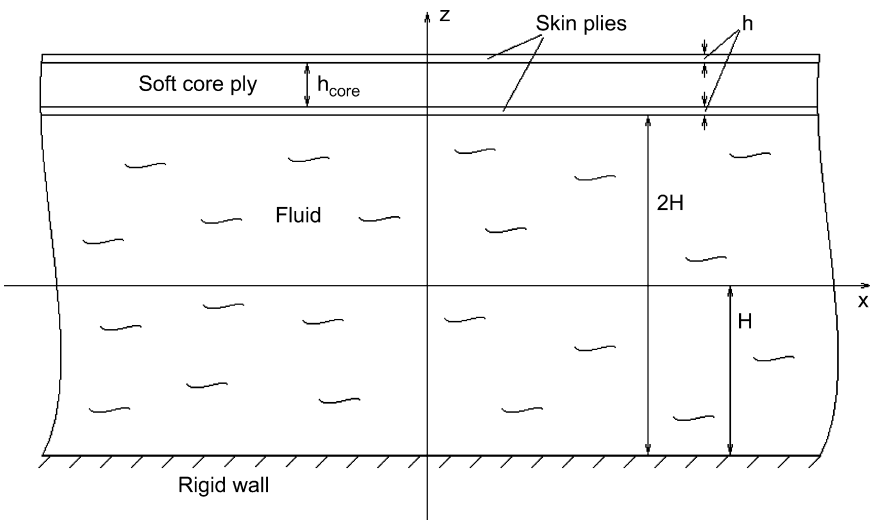

Fig. 5. A fluid-loaded sandwich plate.

The elastic parameters in Eqs. (35) are ($E \equiv E_{\text{skin}}$, $h \equiv h_{\text{skin}}$, $\rho_{\text{pl}} \equiv \rho_{\text{skin}}$)

$$D_1 = \frac{Eh^3}{12(1-\nu_p^2)}\left(2+\frac{\gamma}{\varepsilon^3}\right) = Eh^3\bar{D}_1, \quad D_2 = \frac{Eh^3}{2(1-\nu_p^2)}\left(1+\frac{1}{\varepsilon}\right)^2 = Eh^3\bar{D}_2,$$
$$\Gamma = \frac{Eh}{2(1+\nu_p)}\left(1+\frac{1}{\varepsilon}\right)^2\gamma_g\varepsilon = Eh\bar{\Gamma}, \quad M = \rho_{\text{pl}}h\left(2+\frac{\delta}{\varepsilon}\right) = \rho_{\text{pl}}h\bar{M},$$
$$I_1 = \frac{\rho_{\text{pl}}h^3}{12}\left(2+\frac{\delta}{\varepsilon^3}\right) = \rho_{\text{pl}}h^3\bar{I}_1, \quad I_2 = \frac{\rho_{\text{pl}}h^3}{12}\left(1+\frac{1}{\varepsilon}\right)^2 = \rho_{\text{pl}}h^3\bar{I}_2,$$
$$N_1 = h\left(1+\frac{1}{2\varepsilon}\right) = h\bar{N}_1. \tag{36}$$

Dynamics of the fluid is governed by Eqs. (7) and (8), with continuity condition at the fluid–structure interface, $z = H$, written in the form

$$\begin{cases} v_x = \dfrac{\partial\varphi}{\partial x} - \dfrac{\partial\psi}{\partial z} = N_1\left(\dfrac{\partial^2 w}{\partial t\,\partial x} + \dfrac{\partial\theta}{\partial t}\right), \\ v_z = \dfrac{\partial\varphi}{\partial z} + \dfrac{\partial\psi}{\partial x} = \dfrac{\partial w}{\partial t}. \end{cases} \tag{37}$$

The second pair of conditions at $z = -H$ is the same as in two previous cases. It is given by Eq. (14).

A solution of the problem (7), (8), and (35)–(37) is sought in the form

$$\varphi = A(z)\exp(kx - \mathrm{i}\omega t), \quad \psi = B(z)\exp(kx - \mathrm{i}\omega t),$$
$$w = D\exp(kx - \mathrm{i}\omega t), \quad \theta = F\exp(kx - \mathrm{i}\omega t). \tag{38}$$

Standard algebra gives the following dispersion equation in non-dimensional form

$$T_1 - \frac{\mathrm{i}\Delta^2 P\Omega\mu}{12\chi S}T_2 + \frac{\bar{N}_1^2 P^2\Omega^2\mu^2}{48\chi^2 S^2}T_3 = 0. \tag{39}$$

It is solved by the same method as Eqs. (18), (19) and (21). Cumbersome coefficients involved in Eq. (39) can be found in the Appendix.

Dispersion curves are presented in Fig. 6a and b for following parameters set $\varepsilon = 0.25$, $\gamma = 0.0001$, $\delta = 0.1$ and $\nu_p = 0.3$. This combination of parameters is typical for a plate made of thin steel skins and PVC core (see Ref. [21]). Fluid loading parameters are $P = 0.128$, $\Delta = 3.258$, $\chi = 10$, $\mu = 10^{-6}$. Dispersion curves for the sandwich plate loaded by the acoustic medium are almost identical to those presented in Fig. 6. Dispersion equation for this model (sandwich plate—acoustic medium) is

$$T_1 + \frac{1}{\chi}P\Omega^2\frac{\cot(2\sqrt{K^2+\Omega^2})}{\sqrt{K^2+\Omega^2}}\left(\frac{\Delta^2}{\chi^2}\bar{D}_2K^2 - \Delta^2\bar{\Gamma} + \frac{1}{\chi^2}\bar{I}_2\Omega^2\right) = 0. \tag{40}$$

Figs. 3 and 6 are rather similar, but (unlike the case of a conventional plate) curves 2 and 10 have appeared in Fig. 6. They correspond to the second structure-originated dominantly shear mode. It cuts on at $\Omega \approx 0.32$. The cut-on frequency of the first fluid-originated mode for a sandwich plate ($\Omega \approx 0.44$) becomes smaller than in the case of a Kirchhoff plate ($\Omega \approx 0.5745$). The 'crossing' or 'veering' zone of curves 10 and 11 is zoomed in Fig. 6c and d (real and imaginary parts). As is seen, these two curves in Fig. 6d actually do not intersect each other, but their modes are 'swapped' at the point 'A'. This is a very well-known effect (see, for example, Ref. [22]). As expected, real parts of these curves (see Fig. 6c) also 'swap' at the point A—'attenuation curve' 11 (see also Section 5) of a fluid-originated mode becomes 'attenuation curve' 10 of structure-originated shear mode and vice versa.

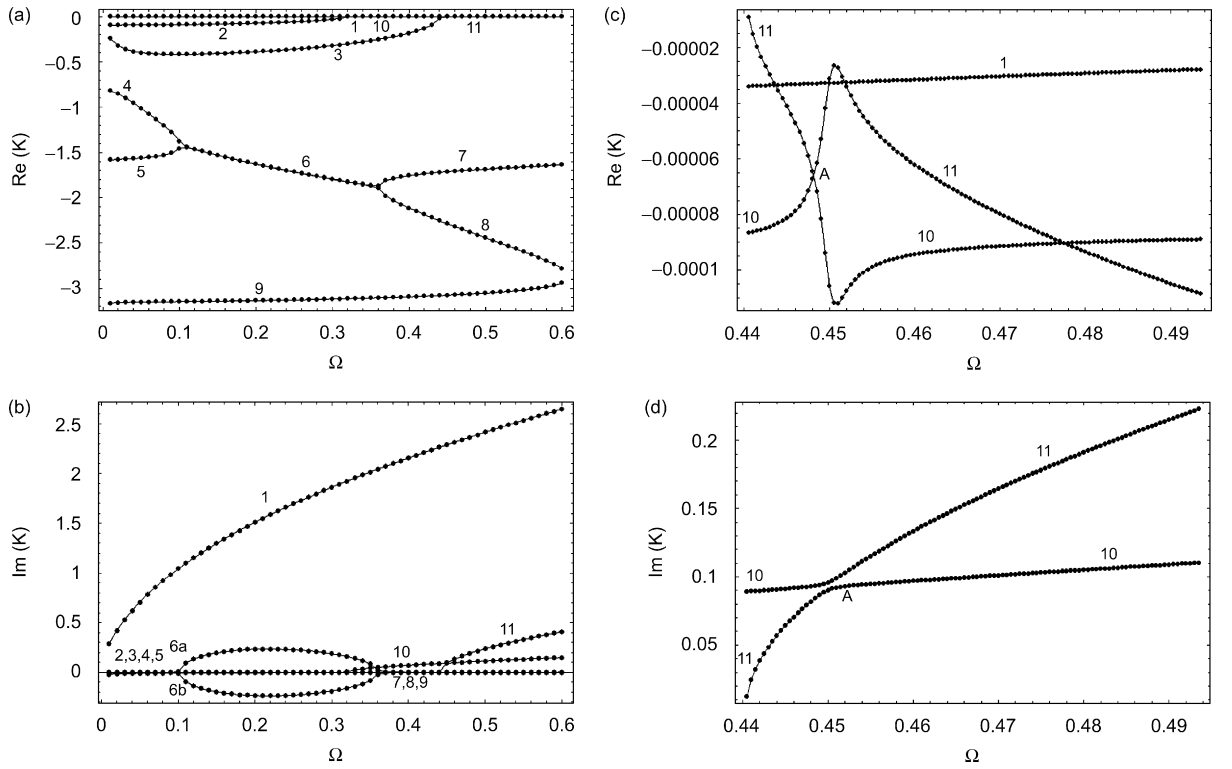

Fig. 6. Dispersion curves for a fluid-loaded sandwich plate: (a) real parts; (b) imaginary parts; (c) real parts zoomed; and (d) imaginary parts zoomed.

The magnitudes of cut-on frequencies can be found from relatively simple equations, which are obtained by setting $K = 0$ in Eqs. (39) and (40):

- in the 'acoustic medium' case:

$$\left(\bar{\Gamma}\Delta^2 - \frac{\bar{I}_2\Omega^2}{\chi^2}\right)\left(-\frac{\bar{M}\Omega^2}{\chi} + P\sqrt{\Omega^2}\,\cot\left(2\sqrt{\Omega^2}\right)\right) = 0. \tag{41a}$$

- in the 'viscous fluid' case:

$$\left(\left(\bar{\Gamma}\Delta^2 - \frac{\bar{I}_2\Omega^2}{\chi^2}\right) + \frac{1}{\chi}\frac{\sqrt{2}}{2}(1-\mathrm{i})\bar{N}_1^2 P\mu^{1/2}\Omega^{3/2}\,\cot\left(2\sqrt{\mathrm{i}\Omega/\mu}\right)\right) \times\left(-\frac{\bar{M}\Omega^2}{\chi} + P\sqrt{\Omega^2}\,\cot\left(2\sqrt{\Omega^2}\right)\frac{3-2\mathrm{i}\mu\Omega}{3}\right) = 0. \tag{41b}$$

Setting to zero the first multiplier in both these formulas yields the equation to determine the cut-on frequency for structure-originated dominantly shear wave. The second one determines cut-on frequencies for fluid-originated modes. As is seen, in the 'acoustic' case the cut-on frequency of the shear wave is linearly dependant upon the 'depth' parameter χ, whereas cut-on frequencies of fluid-originated modes increase slower as χ grows. Cut-on frequencies in 'acoustic medium' and 'viscous fluid' cases are fairly close to each other, when the viscosity parameter μ is sufficiently small. Comparison of Eqs. (31), (34), (41a,b) shows that fluid-originated modes have smaller cut-on frequencies in the sandwich plate case than in the Kirchhoff plate case for the same χ. This fact can also be observed in comparison of Figs. 3 and 6.

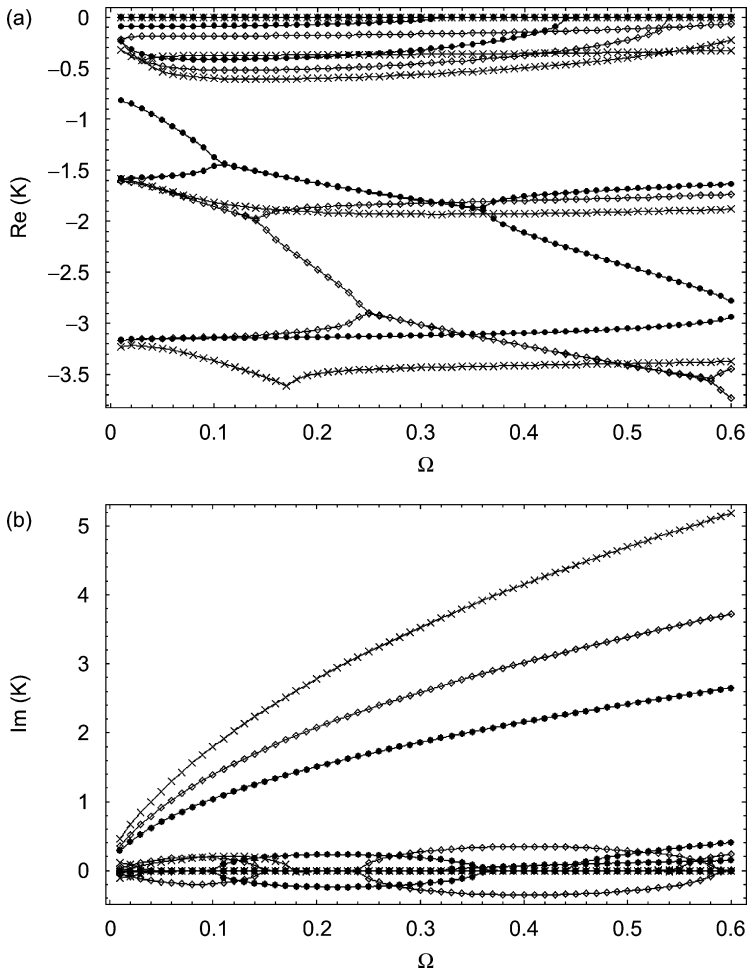

Fig. 7. Dispersion curves obtained for three magnitudes of the depth parameter χ: (a) real parts and (b) imaginary parts.

The influence of parameters χ, ε and γ on shape and location of dispersion curves is illustrated in Figs. 7–9. The influence of the depth parameter χ is illustrated in Fig. 7. Curves designated by dots are plotted for $\chi = 10$, by boxes for $\chi = 20$ and by daggers for $\chi = 40$. This parameter influences cut-on frequencies of structure-originated shear mode and fluid-originated modes. The influence of the geometry parameter ε is illustrated in Fig. 8. Curves designated by dots are plotted for $\varepsilon = 0.15$, by boxes for $\varepsilon = 0.25$ and by daggers for $\varepsilon = 1$. This parameter mainly influences cut-on frequencies for structure-originated shear wave. Finally, the influence of the stiffness parameter γ is illustrated in Fig. 9. Curves denoted by dots correspond to $\gamma = 0.0001$, by boxes to $\gamma = 0.0005$ and by daggers to $\gamma = 0.0025$.

5. Wave attenuation in a sandwich plate loaded by a layer of viscous compressible fluid

The analysis presented in the previous section has been aimed at identification of different types of 'almost propagating' waves. However, from the practical viewpoint, it is important to assess the decay of these waves as they travel a certain distance along the wave guide (a fluid-loaded sandwich plate). Let an incident wave have the amplitude A_{in} at the 'entry' to the wave guide of the length L and the width $2H$. Due to fluid viscosity, this wave is attenuated and its amplitude becomes A_{out} at its outlet. The ratio of these amplitudes characterizes

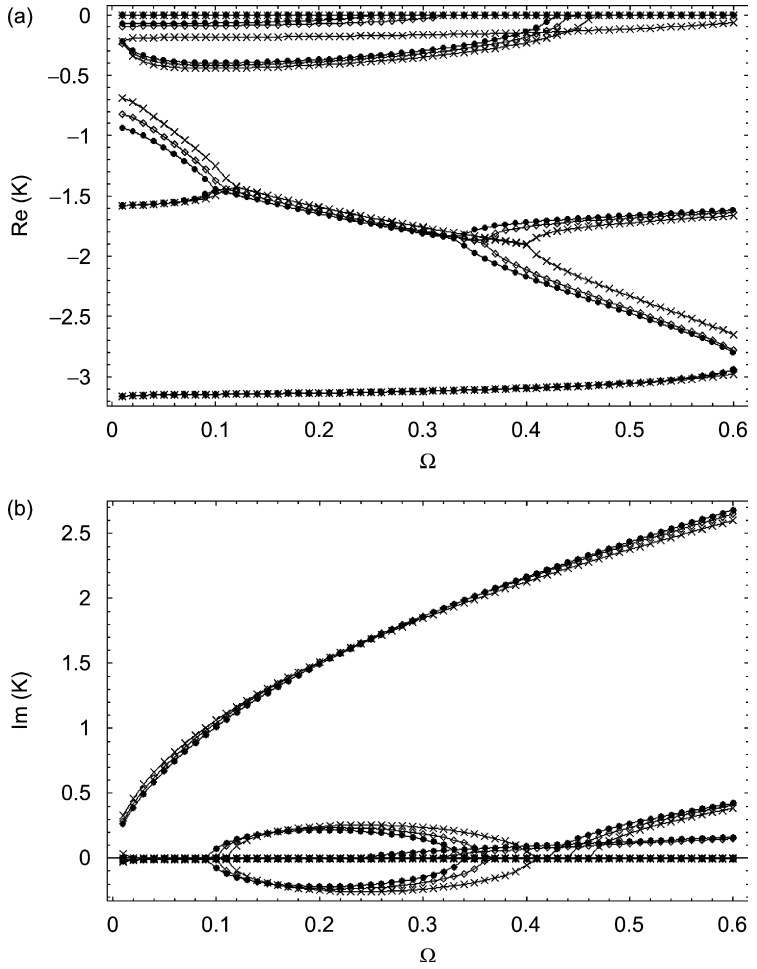

Fig. 8. Dispersion curves obtained for three magnitudes of the geometry parameter ε: (a) real parts and (b) imaginary parts.

the viscosity-induced decay,

$$\frac{A_{\text{out}}}{A_{\text{in}}} = \exp\left(\frac{L}{2H}\operatorname{Re} K\right), \quad \operatorname{Re} K < 0. \tag{42}$$

As is seen from Eq. (42), the level of wave attenuation is controlled by the magnitude of the real part of K.

The following notations are used in all figures presented in this section: curve A—structure-originated 'flexural' modes, curve B—structure-originated 'shear' modes, curve C—first fluid-originated modes, and curve D—second fluid-originated modes. Curves denoted by dots in Fig. 10 correspond to the magnitude of the depth parameter $\chi = 10$, by boxes to $\chi = 20$ and by daggers to $\chi = 40$. The parameters of sandwich plate composition are $\varepsilon = 0.25$, $\gamma = 0.0001$, $\delta = 0.1$. It is supposed that variation of χ is achieved by variation of the thickness of a plate h, since in this figure the following scaling is used: $K = kH$, $\Omega = \omega H/c_{\text{fl}}$. The depth parameter χ has significant influence on the attenuation of structure-originated mode (the increase in χ, produced by the decrease in the thickness of a plate, h, leads to more efficient attenuation). On the other hand, it weakly influences attenuation of the fluid-originated modes. In Fig. 11, designation of curves is similar to Fig. 10, but here it is supposed that the depth of a fluid layer H varies to achieve changes in the magnitude of the depth parameter χ, whereas the thickness of a skin ply does not vary. Curves denoted by dots correspond to $\chi = 10$, by boxes to $\chi = 20$ and by daggers to $\chi = 25$. In this figure, the 'standard' scaling $K = kh$, $\Omega = \omega H/c_{\text{pl}}$ is recovered. As expected, large thickness of fluid layer induces more intensive attenuation of fluid-originated modes (curves C). As is also seen from this figure, there is a very insignificant influence of this

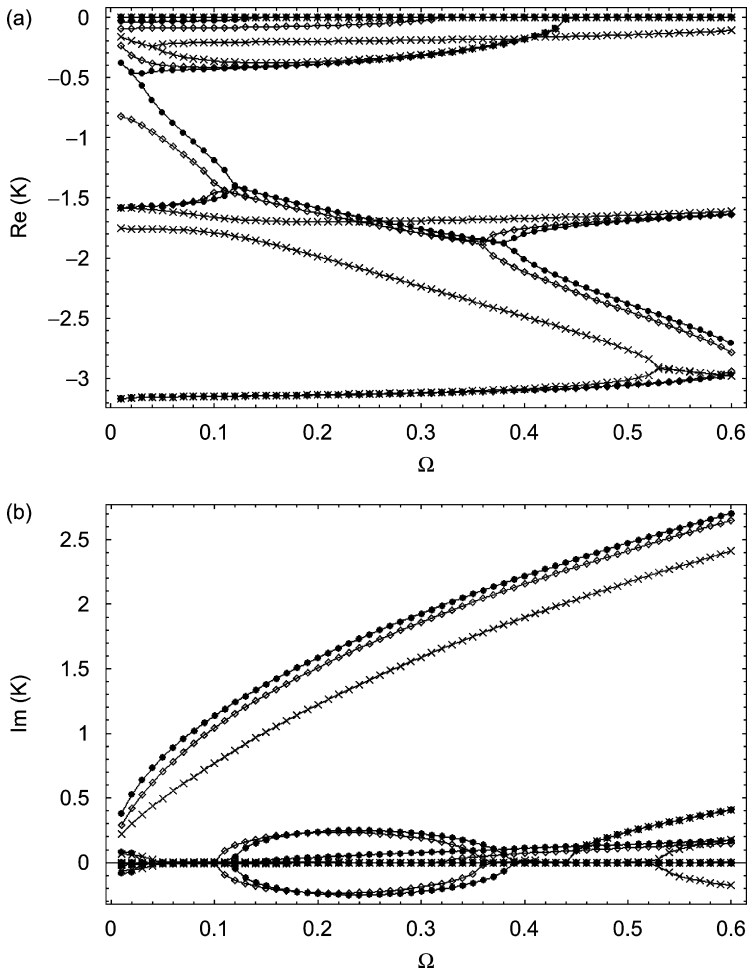

Fig. 9. Dispersion curves obtained for three magnitudes of the stiffness parameter γ: (a) real parts and (b) imaginary parts.

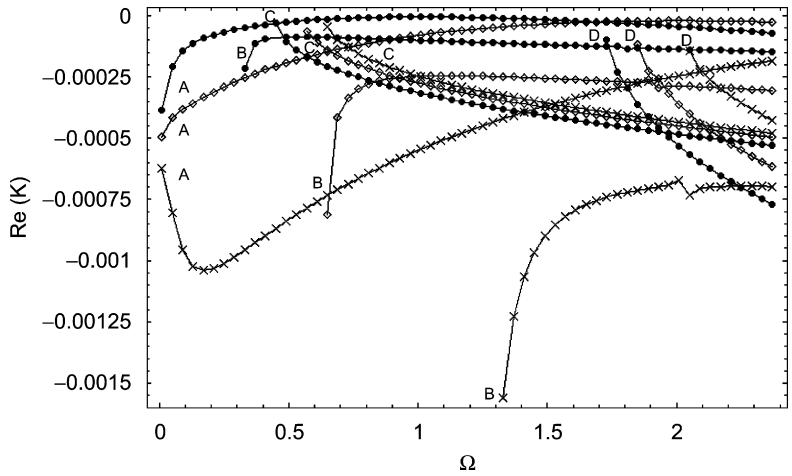

Fig. 10. Real parts of wavenumbers of viscosity-attenuated waves for various magnitudes of the depth parameter χ (H is kept constant), sandwich plate.

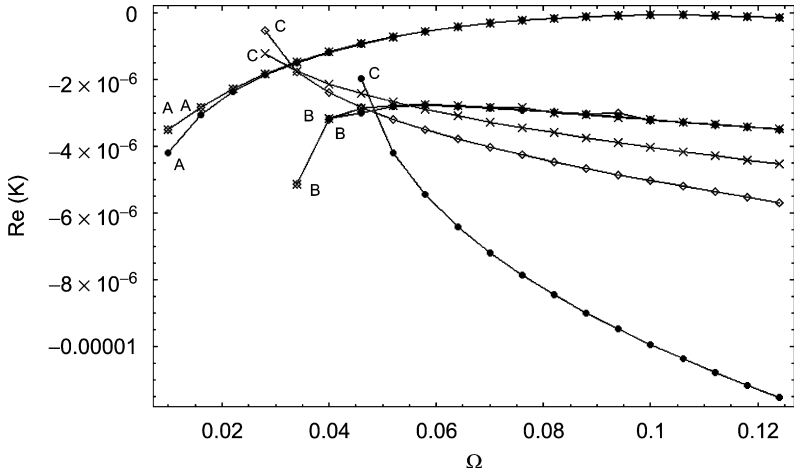

Fig. 11. Real parts of wavenumbers of viscosity-attenuated waves for various magnitudes of the depth parameter χ (h is kept constant), sandwich plate.

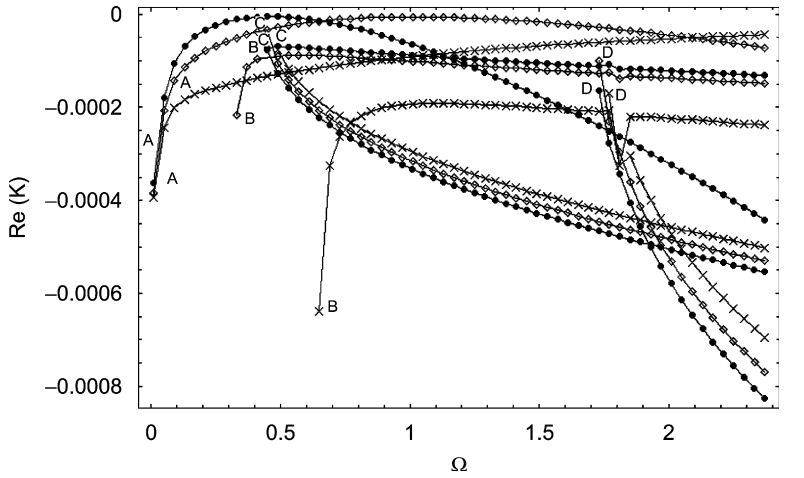

Fig. 12. Real parts of wavenumbers of viscosity-attenuated waves for various magnitudes of the geometry parameter ε, sandwich plate.

parameter on attenuation of structure-originated modes (location of A and B curves is virtually not affected by variation in χ).

The influence of the geometry parameter ε is illustrated in Fig. 12. Other parameters of sandwich plate composition are $\gamma = 0.0001$, $\delta = 0.1$. The depth parameter is set to $\chi = 10$. Curves denoted by dots correspond to $\varepsilon = 0.15$, by boxes to $\varepsilon = 0.25$ and by daggers to $\varepsilon = 1$. As is seen, the rate of decay is not a monotonous function of the frequency parameter for the first structure-originated mode (curves A). For each magnitude of the geometry parameter, it is possible to indicate a frequency, at which attenuation is minimal. This phenomenon can be readily explained by inspection into the dependence of modal coefficients of the considered wave upon frequency. These modal coefficients define 'proportion', in which the structure and the fluid are involved in formation of the wave in the coupled system. The participation of fluid motion is minimal exactly at the frequency, which yields the minimum in attenuation. Finally, the influence of stiffness parameter γ is illustrated in Fig. 13. Curves designated by dots correspond to $\gamma = 0.0001$, by boxes to $\gamma = 0.0005$ and by daggers to $\gamma = 0.0025$. Other parameters are $\varepsilon = 0.25$, $\delta = 0.1$ and $\chi = 10$. The stiffness parameter γ has significant influence only on the shear-mode cut-on frequencies (and on attenuation of corresponding modes).

To have a practical assessment of the decay rate of different waves, consider a sandwich plate with steel skins of thickness 0.5 mm with a PVC core of thickness 2 mm. A layer of viscous compressible fluid has the width of 5 mm. The attenuation distance is taken to be 1 m along the plate. The fluids are selected as petrol,

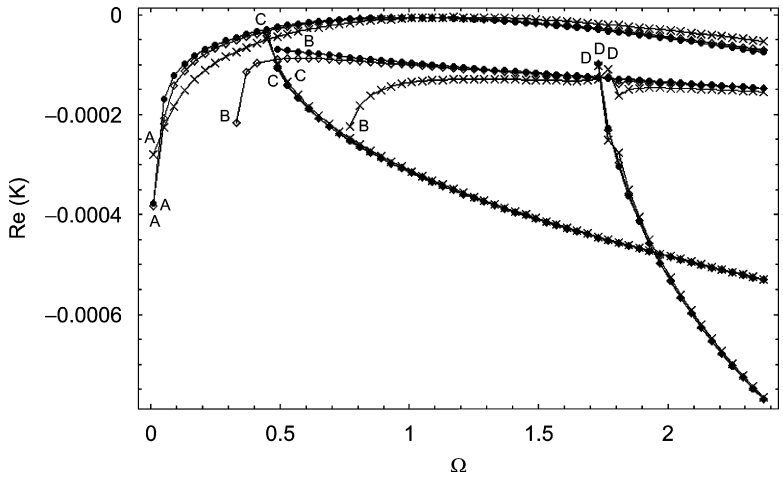

Fig. 13. Real parts of wavenumbers of viscosity-attenuated waves for various magnitudes of the stiffness parameter γ, sandwich plate.

Table 1
Free wave attenuation rate

Fluid	Kinematic viscosity (cSt)	Structure-originated flexural wave (%)	Structure-originated shear wave (%)	Fluid-originated wave (%)
Petrol	6.8636×10^{-7}	0.02	2.41	8.68
Water	9.32039×10^{-7}	0.31	3.95	10.1
Acetone	1.6535×10^{-6}	0.32	2.82	12.93
Olive oil	0.00009	6.67	24.74	62.76
Glycerine	0.000718	45.55	68.97	77.36

water, acetone, olive oil and glycerine. The frequency is selected as 35.5 kHz to ensure co-existence of three propagating waves in a wave guide (A-, B- and C-waves in the terminology of this section). The decay rate in percent for each of these waves is presented in Table 1. As is seen from this data, the fluid-originated wave is attenuated more severely than all other ones in the same excitation conditions. This is an obvious result. As is also expected, the attenuation of the shear wave is always stronger than the attenuation of the flexural wave, because the shear mode has larger involvement of fluid motion, than the flexural mode. As can be seen, a fluid of low viscosity (e.g., water) produces weak attenuation. Nonetheless, there might be cases, when even decay in a few percent in the amplitude of a wave, which is expected to be purely travelling, is important. Highly viscous fluids produce very substantial attenuation of waves of all types. It should also be observed that a layer of viscous compressible fluid with 'lubrication-size' width would certainly produce significant suppression of the wave propagation.

6. Conclusions

The problem of wave propagation in an elastic structure under heavy fluid loading is typically formulated within the framework of the classical model of an acoustic medium. However, in the cases when fluid occupies a long narrow gap between two parallel or co-axial rigid and/or elastic surfaces, this model is inadequate because the attenuation of a travelling wave due to fluid viscosity becomes substantial. This phenomenon is modelled and analysed in this paper. It is found that even in the case of water-loaded structures, the attenuation of 'almost propagating' waves may be noticeable and the level of attenuation is influenced differently by various parameters involved in the problem formulation. The viscosity-induced attenuation becomes more significant in the case of a fluid-loaded sandwich plate, than in the case of a conventional plate, because sandwich composition inflicts a strong fluid–structure coupling due to its relatively high compliance to

tangential 'sliding' deformation. As soon as more 'exotic' fluids, than water, are concerned, the wave attenuation may reach very high level. The reported methodology may readily be extended to capture the energy dissipation within material of the plate (which can be rather large in the core ply of the sandwich plate), but the energy dissipation in the viscous fluid assessed in this paper should remain the same.

Appendix. Coefficients in dispersion equations

1. Coefficients in dispersion equation (29) for a Kirchhoff plate loaded by viscous fluid:

$$T_1 = \frac{\Delta^2}{\chi^3} K^4 \bar{D}_1 - \frac{1}{\chi}\Omega^2,$$

$$T_2 = 2\left(2\alpha^2 + 4K^2 + 3\mathrm{i}\frac{\Omega}{\mu}\right)\left(\frac{K^2}{\chi}S_{11} - 2\beta S_{12}\right) - 3\frac{K^2}{\chi}(\beta^2 + K^2)\left(\frac{\alpha}{\chi}S_{21} + 2S_{22}\right) - 6\frac{K^2\alpha}{\chi}\left(\frac{K^2}{\chi}S_{31} + 2\beta S_{32}\right) + 12\beta K^2\left(\frac{\alpha}{\chi}S_{41} + 2S_{42}\right),$$

$$S = (\alpha\beta\cos\alpha\sin\beta - K^2\sin\alpha\cos\beta)(\alpha\beta\sin\alpha\cos\beta - K^2\cos\alpha\sin\beta),$$

$$S_{11} = -\alpha\beta(\cos 2\alpha\cos 2\beta - 1) - K^2\sin 2\alpha\sin 2\beta,$$

$$S_{12} = -\alpha\beta\cos 2\alpha\sin 2\beta + K^2\sin 2\alpha\cos 2\beta,$$

$$S_{21} = -(-\alpha\beta\sin 2\alpha\cos 2\beta + K^2\cos 2\alpha\sin 2\beta),$$

$$S_{22} = -(-\alpha\beta(\cos 2\alpha\cos 2\beta - 1) - K^2\sin 2\alpha\sin 2\beta),$$

$$S_{31} = -\alpha\beta\sin 2\alpha\cos 2\beta + K^2\cos 2\alpha\sin 2\beta,$$

$$S_{32} = \alpha\beta\sin 2\alpha\sin 2\beta + K^2(\cos 2\alpha\cos 2\beta - 1),$$

$$S_{41} = -(\alpha\beta\sin 2\alpha\sin 2\beta + K^2(\cos 2\alpha\cos 2\beta - 1)),$$

$$S_{42} = -(\alpha\beta\cos 2\alpha\sin 2\beta - K^2\sin 2\alpha\cos 2\beta),$$

$$\chi = \frac{H}{h}, \quad P = \frac{\rho_{\mathrm{fl}}}{\rho_{\mathrm{pl}}}, \quad \Delta = \frac{c_{\mathrm{pl}}}{c_{\mathrm{fl}}}.$$

2. Coefficients in dispersion equation (39) for a sandwich plate loaded by viscous fluid:

$$T_1 = \frac{\Delta^4}{\chi^6}K^6\bar{D}_1\bar{D}_2 - \frac{\Delta^4}{\chi^4}K^4\bar{\Gamma}(\bar{D}_1 + \bar{D}_2) + \frac{\Delta^2}{\chi^6}K^4\Omega^2(\bar{D}_2\bar{I}_1 + \bar{D}_1\bar{I}_2) - \frac{\Delta^2}{\chi^4}K^2\Omega^2(\bar{\Gamma}\bar{I}_1 + \bar{\Gamma}\bar{I}_2 + \bar{M}\bar{D}_2) + \frac{1}{\chi^6}K^2\Omega^4\bar{I}_1\bar{I}_2 + \frac{\Delta^2}{\chi^2}\bar{M}\bar{\Gamma}\Omega^2 - \frac{1}{\chi^4}\bar{M}\bar{I}_2\Omega^4,$$

$$
\begin{aligned}
T_2 = {} & \left(2\alpha^2 + 4K^2 + 3\mathrm{i}\frac{\Omega}{\mu}\right)\left(\bar{\Gamma}\beta S_{12} + \frac{1}{\chi^2}\left(-S_{12}\beta + \frac{\bar{N}_1 K^2 S_{11}}{\chi}\right)\left(\bar{D}_2 K^2 + \bar{I}_2\frac{\Omega^2}{\Delta^2}\right)\right) \\
& + 6\beta K^2\left(-\bar{\Gamma}S_{42} + \frac{1}{\chi^2}\left(S_{42} + \frac{\bar{N}_1\alpha S_{41}}{\chi}\right)\left(\bar{D}_2 K^2 + \bar{I}_2\frac{\Omega^2}{\Delta^2}\right)\right) \\
& - 6\bar{N}_1\frac{\alpha}{\chi^2}K^2\left(\frac{1}{\chi}\beta S_{32}\left(\bar{D}_2 K^2 + \bar{I}_2\frac{\Omega^2}{\Delta^2}\right) + \bar{N}_1 S_{31}\left(\frac{1}{\chi^2}(\bar{D}_1 + \bar{D}_2)K^4 + \left(\frac{K^2}{\chi^2}(\bar{I}_1 + \bar{I}_2) - \bar{M}\right)\frac{\Omega^2}{\Delta^2}\right)\right) \\
& - 3\bar{N}_1\frac{1}{\chi^2}(\beta^2 + K^2)\left(\frac{1}{\chi}K^2 S_{22}\left(\bar{D}_2 K^2 + \bar{I}_2\frac{\Omega^2}{\Delta^2}\right) + \bar{N}_1\alpha S_{21}\left(\frac{1}{\chi^2}(\bar{D}_1 + \bar{D}_2)K^4 + \left(\frac{K^2}{\chi^2}(\bar{I}_1 + \bar{I}_2) - \bar{M}\right)\frac{\Omega^2}{\Delta^2}\right)\right), \\
T_3 = {} & -6\alpha\beta K^2((\beta^2 + K^2)(S_{22}S_{41} - S_{21}S_{42}) + 2(-K^2 S_{31}S_{42} + \alpha\beta S_{32}S_{41})) \\
& + (-2\alpha\beta K^2(S_{12}S_{31} + S_{11}S_{32}) - (\beta^2 + K^2)(K^2 S_{11}S_{22} + \alpha\beta S_{12}S_{21}))\left(2\alpha^2 + 4K^2 + 3\mathrm{i}\frac{\Omega}{\mu}\right).
\end{aligned}
$$

References

[1] D.G. Crighton, A.P. Dowling, J.E. Ffowcs Williams, M. Heckl, F.G. Leppington, *Modern Methods in Analytical Acoustics. Lecture notes*, Springer, Berlin, 1992.

[2] M.G. Junger, D. Feit, *Sound, Structures and their Interaction*, second ed., MIT Press, Cambridge, MA, 1993.

[3] A.N. Guz, Dynamics of solid bodies in a compressible viscous quiescent fluid, *Prikladnaya Mekhanika* 18 (1981) 3–22 (in Russian).

[4] S.G. Kadyrov, J. Wauer, S.V. Sorokin, A potential technique in the theory of interaction between a structure and a viscous, compressible fluid, *Archive of Applied Mechanics* 71 (2001) 405–417.

[5] C.L. Morfey, The role of viscosity in aerodynamic sound generation, *Aeroacoustics* 2 (2003) 225–240.

[6] S.N. Gurbatov, O.V. Rudenko (Eds.), *Problems in Acoustics*, Nauka, Fizmatlit, 1996 (in Russian).

[7] S.V. Sorokin, O.A. Ershova, Plane wave propagation and frequency band gaps in periodic plates and cylindrical shells with and without heavy fluid loading, *Journal of Sound and Vibration* 278 (2004) 501–526.

[8] S.V. Sorokin, Analysis of vibrations and energy flows in sandwich plates bearing concentrated masses and spring-like inclusions in heavy fluid loading conditions, *Journal of Sound and Vibration* 253 (2002) 485–505.

[9] F. Peng, H. Liu, S.Y. Hu, Love wave propagation in a layered piezoelectric structure immersed in a viscous fluid, *Key Engineering Materials* 307 (2006) 1211–1216.

[10] B. McCarthy, G.G. Adams, N.E. McGruer, A dynamic model, including contact bounce, of an electrostatically actuated microswitch, *Journal of Microelectromechanical Systems* 11 (2002) 276–283.

[11] L.M. Milne-Thompson, *Theoretical Hydrodynamics*, fifth ed., Dover, New York, 1996.

[12] L.D. Landau, E.M. Livshitz, *Fluid Mechanics*, second ed., Pergamon Press, Oxford, 1987.

[13] S. Wolfram, *Mathematica: a System for Doing Mathematics by Computer*, Addison-Wesley Publishing Co., Reading, MA, 1991.

[14] C.J. Chapman, S.V. Sorokin, The forced vibration of an elastic plate under significant fluid loading, *Journal of Sound and Vibration* 281 (2005) 19–741.

[15] A.J. Hull, Analysis of a fluid-loaded thick plate, *Journal of Sound and Vibration* 279 (2005) 497–507.

[16] S.V. Sorokin, Analysis of time harmonic wave propagation in an elastic layer under heavy fluid loading, *Journal of Sound and Vibration* 305 (2007) 689–702.

[17] J.D. Smith, Symmetric wave corrections to the liner driven, fluid loaded, thin elastic plate, *Journal of Sound and Vibration* 305 (2007) 827–842.

[18] F. Fahy, *Sound and Structural Vibration, Radiation, Transmission and Response*, Academic Press, New York, 1989.

[19] A. Sarkar, V.R. Sonti, An asymptotic analysis for the coupled dispersion characteristics of a structural acoustic waveguide, *Journal of Sound and Vibration* 306 (2007) 657–674.

[20] A.P. Filin, *Applied Mechanics of Deformable Bodies*, Vol. 1, Nauka, Moscow, 1978 (in Russian).

[21] D. Zenkert (Ed.), *The Handbook of Sandwich Construction*, EMAS Publ., 1997.

[22] R.J. Briggs, *Electro-Stream Interaction with Plasmas*, MIT Press, Cambridge, MA, 1964.